EARTHQUAKE ENGINEERING AND STRUCTURAL DYNAMICS
Earthquake Engng. Struct. Dyn. **27**, 1315–1330 (1998)

A STUDY OF FIXED-ORDER MIXED NORM DESIGNS FOR A BENCHMARK PROBLEM IN STRUCTURAL CONTROL

MARK S. WHORTON[1,*,†], ANTHONY J. CALISE[2,‡] AND C.-C. HSU[2,§]
[1] *ED12/Precision Pointing Control Systems, NASA/Marshall Space Flight Center, Huntsville, Alabama, U.S.A.*
[2] *School of Aerospace Engineering, Georgia Institute of Technology, Atlanta, Georgia, U.S.A.*

SUMMARY

This study investigates the use of H_2, μ-synthesis, and mixed H_2/μ methods to construct full-order controllers and optimized controllers of fixed dimensions. The benchmark problem definition is first extended to include uncertainty within the controller bandwidth in the form of parametric uncertainty representative of uncertainty in the natural frequencies of the design model. The sensitivity of H_2 design to unmodelled dynamics and parametric uncertainty is evaluated for a range of controller levels of authority. Next, μ-synthesis methods are applied to design full-order compensators that are robust to both unmodelled dynamics and to parametric uncertainty. Finally, a set of mixed H_2/μ compensators are designed which are optimized for a fixed compensator dimension. These mixed norm designs recover the H_2 design performance levels while providing the same levels of robust stability as the μ designs. It is shown that designing with the mixed norm approach permits higher levels of controller authority for which the H_2 designs are destabilizing. The benchmark problem is that of an active tendon system. The controller designs are all based on the use of acceleration feedback.

KEY WORDS: robust control; mixed H_2/μ control; parametric uncertainty; homotopy methods; structural control

1. INTRODUCTION

Concepts for active and hybrid active/passive control in building structures have been explored by a number of authors (e.g. Reference 1). More recent attention has been given to the application of robust control theory in the context of H_∞ design (e.g. References 2–4). Robust control is concerned with maintaining performance with uncertainty in the dynamical system. Uncertainties are basically the discrepancies between the mathematical model of the plant to be controlled and the actual plant. It is often the case that the higher modes of vibration of a structure are discarded in the model. Thus, one form of uncertainty is due to neglected dynamics. Another example is the mass or stiffness of some element of the dynamical system, which will always differ to some degree from the model value. This is called parametric uncertainty. Exogenous inputs, or disturbances, are also uncertainties. They affect performance, but not stability. For an actively controlled building, seismic activity, wind gusts, and sensor noise are examples of exogenous disturbances. Robust control means having a controller which maintains stability and performance specifications in the presence of uncertainty. Performance is measured by the response of the controlled system to worst-case bounded

* Correspondence to: Mark S. Whorton, ED12/Precision Pointing Control Systems, NASA/Marshall Space Flight Center, Huntsville, Alabama, U.S.A. E-mail: mark.whorton@msfc.nasa.gov
† Aerospace Engineer
‡ Professor
§ Research Engineer

CCC 0098–8847/98/111315–16$17·50
Received 10 June 1997
Revised 22 November 1997

disturbances. Specific definitions of performance will be given later. Before robust control theory was developed, multivariable controller design techniques provided only sufficient conditions for robust performance, which could be very conservative for poorly conditioned plants (or for well-conditioned plants with non-round performance specifications). What distinguishes robust control theory is that it provides a systematic approach to evaluating and designing controllers that attempt to maintain performance specifications in the presence of uncertainty in a non-conservative fashion. Because robust controllers can tolerate uncertainties, control of a building structure's seismic response is an ideal application. The examples of uncertainties given above are all present. Also, deformations in the structure will cause changes in the inherent stiffness and passive damping. The non-linearities encountered in the deformation of the building structure during a seismic event can also be considered as uncertainties.

While robust control provides performance in the presence of uncertainties, the performance is defined by an H_∞ norm measure, which may not be well suited to the performance objectives. In cases such as minimizing control energy, line-of-sight pointing error, or (as in this paper) minimizing the root-mean-square (rms) vibration response of a structure, the H_2 norm is a better measure of performance. However, it is well known that H_2 design at high control authority levels has very poor robust stability properties. These issues are addressed in the mixed H_2/H_∞ design method. Mixed H_2/H_∞ design seeks to minimize the H_2 norm of one transfer function while satisfying an overbound constraint on the H_∞ norm of another transfer function. Using this approach allows one to design for H_2 nominal performance while maintaining the robust stability provisions of H_∞ design.

The problem from a controls point of view is the need to develop a controller that can reliably accommodate the uncertainty in excitation that is characteristic of earthquakes, while at the same time handle the presence of uncertainties caused by inelastic structural response. The purpose of this paper is to examine design approaches which achieve nominal performance only (H_2), robust performance (μ-synthesis), and nominal performance/robust stability (mixed H_2/μ), applied to the problem of building structural control. The challenge is to achieve the highest attainable level of rms performance for a specified bounded set of uncertainties. This paper provides a brief description of the H_2, μ-synthesis, and mixed H_2/μ design methods, emphasizing the role of uncertainty modelling. A comparison of these controller design techniques is given, using the three-story tendon controlled structure at the National Center for Earthquake Engineering Research.

2. MODELLING FOR DESIGN AND EVALUATION

Design of a high-performance control system is inherently dependent on the availability of an accurate design model and knowledge of associated uncertainties. For structural systems such as the building control benchmark problem, models are typically of higher order than is desirable, especially when frequency-dependent weights are included in the control design. As in the case of this benchmark problem, the complexity of a control system may have constraints that require either reducing the model dimension for control design, reducing the dimension of the control system, or designing optimal controllers of fixed dimension. This paper implements the latter approach. A reduced-order nominal design model will be obtained from the evaluation model in Reference 5. Additionally, a model formulation will be presented which accounts for real parameter uncertainties in the design model.

2.1. Nominal performance design model

A six state nominal design model was obtained by balancing and residualizing the 20 state evaluation model, retaining the modes at 2·268, 7·332, and 12·240 Hz. The generalized plant for H_2 control design is shown in Figure 1. Inputs consist of the ground acceleration disturbance, $\ddot{x}_g$, sensor noise, and the tendon control input, u. Performance outputs include the weighted displacement of the three floors relative to the ground, zp, and the weighted control force, zu. The measurement output, y, is the absolute acceleration of each of the three floors. All units are in volts.

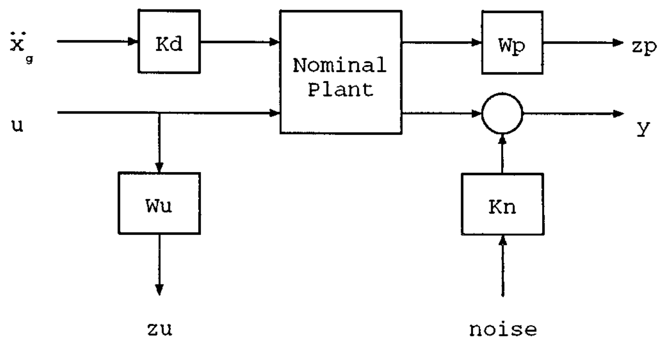

Figure 1. Generalized plant for H_2 control design

2.2. *Robust performance design model*

The nominal evaluation model for the benchmark problem may be extended to include parametric uncertainty within the control bandwidth in the form of errors in the modal damping and frequency squared terms as introduced in Reference 6. Uncertainty will only be used for the natural frequency squared terms in this paper, but for completeness, the formulation for uncertain modal damping will also be presented. Although the uncertain natural frequency square terms are real parameters, using a complex uncertainty also accounts for variations in modal damping if a hysteretic damping model is assumed.

In modal form, the nominal A matrix for a second-order system is written

$$A_0 = \begin{bmatrix} 0 & 1 \\ -\omega^2 & -2\zeta\omega \end{bmatrix} \tag{1}$$

Introducing multiplicative uncertainty in the modal frequency square and modal damping terms results in

$$A = \begin{bmatrix} 0 & 1 \\ -\omega^2(1+\delta_1) & -2\zeta\omega(1+\delta_2) \end{bmatrix} \tag{2}$$

$$= A_0 + \Delta A \tag{3}$$

where

$$\Delta A = \begin{bmatrix} 0 & 0 \\ -\omega^2\delta_1 & -2\zeta\omega\delta_2 \end{bmatrix} \tag{4}$$

$$= \delta_1 \begin{bmatrix} 0 \\ 1 \end{bmatrix} [-\omega^2 \;\; 0] + \delta_2 \begin{bmatrix} 0 \\ 1 \end{bmatrix} [0 \;\; -2\zeta\omega] \tag{5}$$

For a system with n total modes and m uncertain modes, $A = A_0 + \sum_{i=1}^{m} \Delta A_i$, and

$$\Delta A_i = (e_{2i})\delta_{1i}(-\omega_i^2)(e_{2i-1})^{\mathrm{T}} + (e_{2i})\delta_{2i}(-2\zeta_i\omega_i)(e_{2i})^{\mathrm{T}} \tag{6}$$

where (e_j) is the jth standard basis vector for $\Re^{2n}$. Defining k to be the set of indices of uncertain modes allows the plant with uncertain natural frequency square and damping terms to be as shown in Figure 2 with the following definitions:

$$\Delta A_{\mathrm{LW}} = \Delta A_{\mathrm{LD}} = E_{2k}, \quad \Delta A_{\mathrm{RW}} = -\Omega^2 E_{2k-1}^{\mathrm{T}}, \quad \Delta A_{\mathrm{RD}} = -\mathscr{D}\Omega E_{2k}^{\mathrm{T}} \tag{7}$$

$$\Omega = \mathrm{diag}[\omega_{k(i)}], \quad \mathscr{D} = \mathrm{diag}[2\zeta_{k(i)}], \quad \forall i = 1, 2, \ldots, m, \tag{8}$$

$$E_{2k} = [e_{2k(1)} \quad e_{2k(2)} \cdots e_{2k(m)}] \tag{9}$$

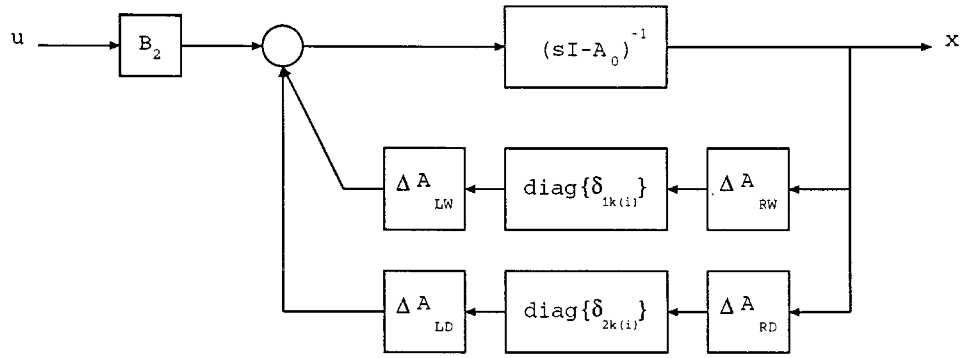

Figure 2. Plant with uncertain modal damping and frequency square terms

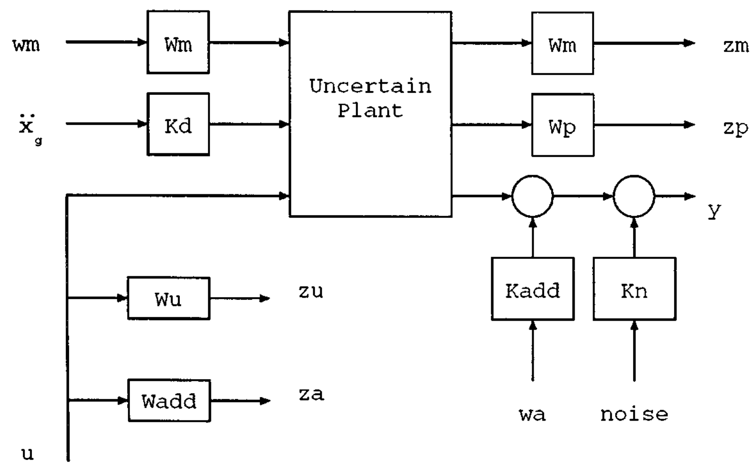

Figure 3. Generalized plant for robust control design

Figure 3 illustrates the generalized plant for robust control design. In addition to the uncertainty in the modal frequency square terms, an additive uncertainty is included to represent model error outside the control bandwidth. This type uncertainty model forces the controller to gain stabilize the high-frequency modes that were truncated from the evaluation model. Additional inputs for the robust control design generalized plant include inputs associated with the additive uncertainty, *wa*, and the modal frequency uncertainty, *wm*. Additional outputs include those associated with the additive uncertainty, *za*, and the modal frequency uncertainty, *zm*.

3. CONTROLLER DESIGN APPROACHES

H_2 methods are often used when designing control systems to reduce the vibration response of a flexible structure. While H_2 design gives good nominal performance, the controllers are highly tuned to the design model and errors in the design model are not accounted for, typically inducing instability at higher levels of control authority. As a result, the actual performance achievable is limited with H_2 designs. To achieve high levels of performance in the actual system, robustness to model errors must be taken into account in the design process. In this section, a brief introduction to H_2, H_∞, μ-synthesis, and mixed H_2/μ control design is given. In the following section, these methods will be used to design controllers for the benchmark structural

control problem and to demonstrate the significance of designing for nominal performance and robust stability. For more details on the theoretical basis of the control design methods used in this paper, see References 7 and 8.

3.1. Design for nominal performance

The generalized plant may be written in state space form as

$$\dot{x} = Ax + B_1 w + B_2 u \tag{10}$$

$$z = C_1 x + D_{12} u \tag{11}$$

$$y = C_2 x + D_{21} w + D_{22} u \tag{12}$$

where $x \in \Re^n$ is the state vector, $w \in \Re^{nw}$ is the disturbance vector, $u \in \Re^{nu}$ is the control vector, $z \in \Re^{nz}$ is the performance vector, and $y \in \Re^{ny}$ is the measurement vector. The H_2 optimization problem is to find a stabilizing controller that minimizes the H_2 norm of the closed-loop system from disturbance inputs w to performance outputs z, denoted T_{zw}. The closed-loop system may also be written as the linear fractional transformation (LFT) shown in Figure 4. Another approach to design for nominal performance employs the H_∞ norm, which can be interpreted as the gain of the system and is the worst-case amplification over all inputs $w(t)$ of unit energy. From a frequency domain perspective, the H_∞ norm is defined as the maximum singular value of $T(s)$ over all frequencies, i.e.

$$\|T_{zw}\|_\infty = \sup_\omega \{\bar{\sigma}(T_{zw}(j\omega))\} \tag{13}$$

H_∞ control design theory, based on References 9 and 10, involves defining (possibly frequency-dependent) weights on the inputs and outputs such that the performance objectives are satisfied by minimizing $\|T_{zw}\|_\infty$. Because the H_∞ norm is defined with respect to the peak magnitude of the transfer matrix frequency response and the H_2 norm is defined by an integral square quantity (in time or frequency by Parseval's Theorem), the respective closed-loop systems may have considerably different characteristics. Depending on the performance objectives, one design procedure may be preferable to the other. With regard to rms performance specifications, H_2 design typically yields better nominal performance. The significant benefit of H_∞ theory is that robustness to model errors is explicitly factored into the design process.

3.2. Design for robust stability

In addition to nominal performance, robust stability is an important design consideration. Robust stability requires the closed-loop system to remain stable for bounded model errors. The uncertainty may be modelled in many forms such as multiplicative, inverse multiplicative, additive, parametric, etc. and may be located at various points in the loop. Recall that in Section 2, a model was presented for the benchmark problem with parametric and additive uncertainty modelled. By absorbing all of the scalings and weights into the plant P, the robust stability problem may be formulated as the LFT in Figure 5. The uncertainties are scaled so that Δ_δ is the set of all stable perturbations such that $\|\Delta\|_\infty \leqslant \delta$. Assuming that $K(s)$ internally stabilizes the closed

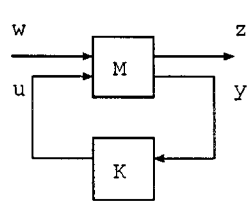

Figure 4. Linear fractional transformation of closed loop

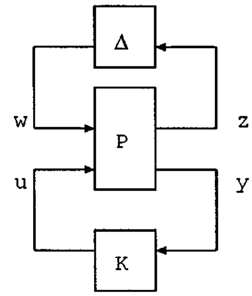

Figure 5. LFT for robust stability analysis

loop for $\Delta = 0$, then a sufficient condition for robust stability for all plants in the set formed by $\Delta \in \Delta_\delta$ is that[11,12]

$$\| T_{zw}(K) \|_\infty \leqslant \frac{1}{\delta} \tag{14}$$

Thus, like the nominal performance problem, robust stability is provided by minimizing the norm of a particular transfer function.

3.3. Design for robust performance

It is the ability to formulate the performance problem as a robust stability problem that enables robust performance controller design in the H_∞ setting. Consider the uncertain plant in Figure 3 with inputs and outputs defined for performance and an uncertainty model. The plant is recast as an LFT in Figure 6, where

$$w_1 = \begin{bmatrix} w_m \\ w_a \end{bmatrix}, \quad w_2 = \begin{bmatrix} \text{noise} \\ \ddot{x}_g \end{bmatrix}, \quad z_1 = \begin{bmatrix} z_m \\ z_a \end{bmatrix}, \quad z_2 = \begin{bmatrix} z_p \\ z_u \end{bmatrix} \tag{15}$$

The conditions for robust performance are:

1. robust stability (equation (14)), and
2. performance maintained for all $\Delta \in \Delta_\delta$.

Closing the loop from z_2 to w_2 through a fictitious uncertainty block Δ_p recasts the robust performance problem as a robust stability problem, shown in Figure 6 where the blocks are scaled to one.

A sufficient condition for robust performance is that

$$\| T(K) \|_\infty < 1 \tag{16}$$

Define $\underline{\Delta}_1$ to be the set of all stable, bounded, unstructured perturbations $\underline{\Delta}$ such that $\|\underline{\Delta}\|_\infty < 1$. When $\underline{\Delta} \in \underline{\Delta}_1$, equation (16) is necessary and sufficient to ensure robust stability. Designing for robust performance using Δ_p as in Figure 6 introduces a block diagonal structure to $\underline{\Delta}$ which results in equation (16) being only sufficient and possibly overly conservative. This conservatism is relaxed in the μ-analysis and μ-synthesis procedures[13–15] by accounting for the block diagonal structure in $\underline{\Delta}$.

The structured singular value is used to define the μ-measure, which although not a norm, is denoted

$$\| T(\mathrm{j}\omega) \|_\mu = \sup_\omega \{ \mu(T_{zw}(\mathrm{j}\omega)) \} \tag{17}$$

Hence the sufficient condition for robust performance in equation (16) becomes the necessary and sufficient condition

$$\| T(\mathrm{j}\omega) \|_\mu < 1 \tag{18}$$

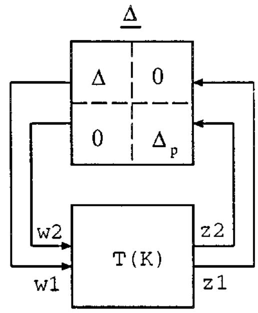

Figure 6. LFT for robust performance design

Although the structured singular value cannot be directly computed, an upper bound can be computed as

$$\mu(T) = \inf_{D} \{\bar{\sigma}(DTD^{-1})\} \tag{19}$$

where $D = \text{diag}[d_j I_j]$ has the same structure as D and d_j are scalar, positive, real functions of frequency. An iterative scheme is used to solve this optimization problem. In the first step, an H_∞ controller is designed and in the second step, the D-scales are optimized for this controller in accordance with equation (19). In the next iteration, these D-scales are incorporated into the generalized plant and the control design is repeated, followed again by D-scaling. This iterative process continues until the upper bound in equation (19) cannot be reduced significantly.

3.4. Design for robust stability and nominal performance

Although μ-synthesis provides stability and performance in the presence of model errors, the performance is defined by an H_∞-norm measure which may yield poor H_2 performance. The mixed H_2/H_∞ design procedure has been developed to provide robust stability and nominal (H_2) performance by minimizing the H_2 norm for one set of inputs/outputs while satisfying an H_∞-norm overbound for another set of inputs/outputs. With reference to Figure 6, the objective is to satisfy

$$\min_{K} \|T_{z2w2}\|_2 \tag{20}$$

subject to

$$\|T_{z1w1}\|_\infty < \gamma \tag{21}$$

This problem has been solved for controllers of fixed dimension[7] with a numerical homotopy algorithm for the formulation of Reference 7 given in Reference 17. The homotopy algorithm that solves the necessary conditions for a fixed-order mixed H_2/H_∞ (or μ) controller is a two-parameter iterative scheme which effectively trades between robust stability and nominal performance by varying the overbound on the H_∞-norm, γ, and the weight on the H_2 cost, λ. For a given γ, λ is increased until the H_∞-norm constraint becomes an active, equality constraint (at which point the H_2 norm can no longer be reduced) or until the H_2 norm ceases to decrease. The set of controllers where the H_∞-norm is equal to the overbound are called the boundary solutions, the set of which provides an explicit trade between nominal performance and robust stability. By incorporating the D-scales from μ-synthesis into the H_∞ subproblem, the structure of the uncertainty block may be accounted for, resulting in a fixed-order mixed H_2/μ design procedure. The next section presents a brief overview of the numerical algorithm used for fixed-order mixed norm controller synthesis.

4. CONTROL DESIGN ALGORITHM

This section presents a brief description of the homotopy algorithm for synthesis of fixed-order mixed H_2/H_∞ controllers (fixed-order H_2 and H_∞ controllers are obtained as special cases). Only an introduction to homotopy methods is presented here, but a complete development of the control design algorithms is given in Reference 17. The formulation and necessary conditions for fixed-order mixed H_2/H_∞ control design is presented in Reference 7 where a controller canonical form is used for the compensator dynamics.

Homotopy methods offer an attractive alternative to more standard approaches of optimal controller synthesis such as sequential and conjugate gradient methods. The basic philosophy of homotopy methods is to deform a problem which is relatively easily solved into the problem for which a solution is desired. Homotopy methods embed a given problem in a parameterized family of problems. More specifically, consider sets Θ and $Y \in \Re^n$ and a mapping $F\colon \Theta \to Y$, where solutions of the problem

$$F(\theta) = 0 \tag{22}$$

are desired with $\theta \in \Theta$ and $F(\theta) \in Y$. The homotopy function is defined by the mapping $H\colon \Theta x[0, 1] \to \Re^n$ such that

$$H(\theta_1, 1) = F(\theta) \tag{23}$$

and there exists a known (or easily calculated) solution, θ_0, such that

$$H(\theta_0, 0) = 0 \tag{24}$$

The homotopy function is a continuously differentiable function given by

$$H(\theta(\alpha), \alpha) = 0, \quad \forall \alpha \in [0, 1] \tag{25}$$

Thus, the homotopy begins with a simple problem with a known solution, equation (24), which is deformed by continuously varying the parameter until the solution of the original problem, equation (22), is obtained.[19] The power of homotopy methods is that minimization is not strongly dependent on starting solution, but depends on local, small variations in the solution. Theoretically, these methods are globally convergent for a wide range of complex optimization problems, but in actuality, finite wordlength computation often introduces numerical ill-conditioning resulting in difficulties with convergence. In light of these numerical limitations, a judicious choice of the initial problem and the associated initial stabilizing compensator is necessary for convergence and efficient computation. However, the ability to select an initial problem with a simple solution renders homotopy methods more widely applicable than sequential or gradient based methods, which have a more stringent requirement for an initial stabilizing solution.

Continuous homotopy methods involve integration of Davidenko's differential equation, which is obtained by differentiating equation (25) with respect to α, yielding

$$\frac{d\theta}{d\alpha} = -\left(\frac{\partial H}{\partial \theta}\right)^{-1} \frac{\partial H}{\partial \alpha} \tag{26}$$

Given $\theta(0) = \theta_0$, this initial value problem may be numerically integrated to obtain the solution at $\alpha = 1$ if the solution exists and is uniquely defined.

In Reference 17, a continuous homotopy algorithm is presented for fixed-order mixed H_2/H_∞ compensator design. The homotopy function is defined as the gradient of the cost functional with respect to the controller parameters. The five first order necessary conditions which result from the mixed norm cost functional include one non-linear, coupled matrix equation (the gradient of the cost functional with respect to the controller parameters), three lyapunov equations, and one ricatti equation. The gradient of the homotopy function is obtained from the second derivative of the mixed norm cost functional and is obtained by differentiating the first order necessary conditions with respect to the controller gain parameters and the homotopy parameter.

In essence, a mixed discrete and continuous approach is employed where Davidenko's differential equation (26), is integrated along the homotopy path and at discrete points along the trajectory, a local optimization is used to remove integration error. Local optimization at discrete points along the homotopy trajectory allows a crude integration procedure with large step sizes to be employed for efficiently tracking the solution curve.

The numerical aspect of fixed-order, mixed norm control design presents quite a challenge for several reasons. For fixed-order control design, there are no guarantees on uniqueness or existence of the fixed-order controllers. Also, use of a canonical form on the controller architecture imposes constraints on the topology of the controller parameter space and may introduce ill-conditioning. Canonical forms are known to be more poorly conditioned, in general, as compared to non-minimal realizations as well. The result is that the numerical algorithm often encounters situations where the hessian is either ill-conditioned (large spread in singular values which may indicate singularity) or indefinite. The existence of local maxima, saddle points, or long narrow valleys provides a severe challenge to local optimization algorithms. A partitioned Newton method was developed for use with the mixed norm homotopy algorithm to accommodate these points where the hessian is ill-conditioned and indefinite.[19]

5. CONTROLLER DESIGN RESULTS

This section presents a comparison of the design approaches for nominal performance (H_2), robust performance (μ-synthesis), and nominal performance/robust stability (mixed H_2/μ) for the benchmark structural control problem. For evaluating the nominal performance of these designs, performance is defined by the rms response of the three relative floor displacements, Vz, and the rms control effort, Vu.

With reference to Figure 1 for the H_2 nominal performance design, the disturbance input and performance output vectors are

$$w = \begin{bmatrix} \text{noise} \\ \ddot{x}_g \end{bmatrix}, \quad z = \begin{bmatrix} z_p \\ z_u \end{bmatrix} \tag{27}$$

The design parameters are defined as follows: the control weight, $Wu = \sqrt{\rho}$, the weight on relative displacement of each floor, $Wp = 25$, the sensor noise intensity, $Kn = 0{\cdot}001$, and the intensity of the ground disturbance, $Kd = 0{\cdot}0017$ (chosen to match the dc intensity of the Kanai-Tajimi (KT) spectrum). Control authority was varied in the design process using the scalar ρ.

For the μ-synthesis design, Figure 3 is used where the uncertainty model included 5 per cent uncertainty for the natural frequency square error ($Wm = \sqrt{0{\cdot}05}$) and the additive uncertainty weighting function is given by

$$W_{\text{additive}} = 6{\cdot}4\,\frac{(s+5)^3}{(s+200)^3} \tag{28}$$

In order to balance the plant for improved numerical results, the additive uncertainty model is realized as the frequency-dependent term, Wadd, and the constant gain term, Kadd, as indicated in Figure 3. The uncertainty block has the structure

$$\Delta = \begin{bmatrix} \delta_1 & & & & \\ & \delta_2 & & 0 & \\ & & \delta_3 & & \\ & 0 & & \Delta_4 & \\ & & & & \Delta_p \end{bmatrix} \tag{29}$$

with $\Delta_4 \in C^{3x1}$ and $\Delta_p \in C^{4x4}$. For the μ-synthesis design, the corresponding disturbance and performance vectors are

$$w = \begin{bmatrix} w_m \\ w_a \\ \text{noise} \\ \ddot{x}_g \end{bmatrix}, \quad z = \begin{bmatrix} z_m \\ z_a \\ z_u \\ z_p \end{bmatrix} \tag{30}$$

A set of μ controllers of varying control authority was designed by fixing Wp and varying ρ to achieve good nominal performance. In order to make a consistent comparison of control approaches from a robustness perspective, each controller was designed to achieve a μ measure of one so that achievable performance given a fixed level of robustness could be evaluated. First-order D-scales were used for each μ controller design, resulting in μ controllers with 19 states computed using the MATLAB μ-Analysis and Synthesis Toolbox.[20]

Finally, a set of mixed H_2/μ controllers were designed with fixed controller dimension of 6th order using the homotopy algorithm of Reference 17. In order to trade between nominal performance and robust stability, the H_2 subproblem is defined for nominal performance as above and the μ subproblem accounts for the additive and parametric uncertainty models. The problems are defined by the inputs and outputs

$$w_1 = \begin{bmatrix} w_m \\ w_a \end{bmatrix}, \quad z_1 = \begin{bmatrix} z_m \\ z_a \end{bmatrix}, \quad w_2 = \begin{bmatrix} \text{noise} \\ \ddot{x}_g \end{bmatrix}, \quad z_2 = \begin{bmatrix} z_p \\ z_u \end{bmatrix} \tag{31}$$

and the D-scales for the μ subproblem are obtained from D–K iterations for T_{z1w1}.

Figure 7 presents the rms nominal performance curves for each control design method. The robust control designs are for the baseline uncertainty model (which has 5 per cent uncertainty in the natural frequency square parameters and the additive uncertainty). The costs are computed with the K–T spectrum input. H_2 design costs are computed for both the design and evaluation models to illustrate the limitation on achievable performance due to model error. Although the cost curve evaluated with the design model extends

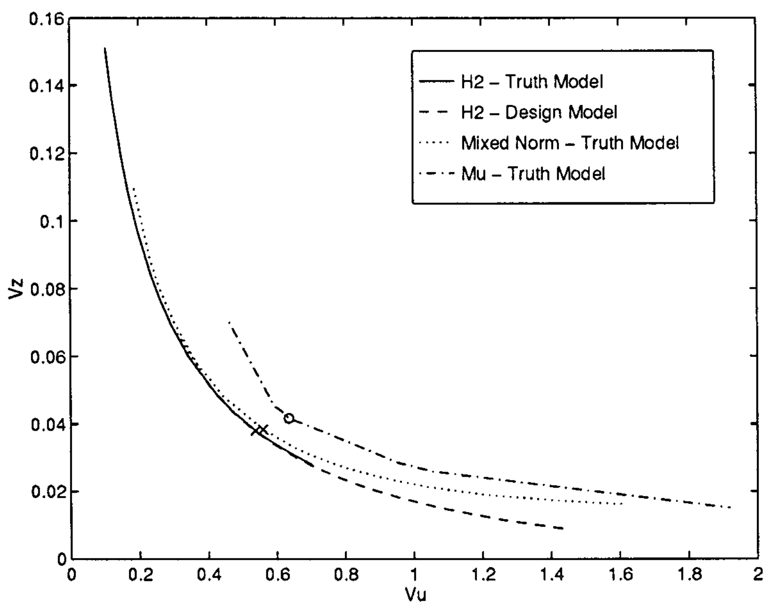

Figure 7. RMS performance comparisons

to high control authority levels, the maximum performance with the evaluation model is obtained at $\rho = 15{\cdot}63$. The loop closed with the H_2 controllers and the evaluation model are unstable for smaller values of ρ. This cost comparison also indicates that for control authority levels lower than the instability level, the actual performance is almost identical to the design model performance.

Figure 7 also indicates the loss of rms performance that is incurred in exchange for robust performance. As a basis for comparison the set of μ designs is evaluated in terms of rms performance. A substantial gap in performance exists between the H_2 and μ designs since the μ designs achieve a given level of output performance at a higher control cost than the H_2 designs. However, the mixed H_2/H_∞ designs effectively recover the rms performance of the H_2 designs while providing the same level of robust stability as the μ designs. The mixed H_2/μ design procedure provides performance comparable to H_2 design while overcoming the major shortcoming of H_2 design, namely a lack of stability robustness.

The impact of uncertainty on performance in the mixed norm design setting is evident in Figure 8 where a set of mixed norm designs are evaluated with 10 and 20 per cent parametric uncertainty in addition to the baseline 5 per cent parametric uncertainty. As the level of robustness increases, performance in sacrificed as indicated by the upward shift in the performance curve. A cursory comparison of Figures 7 and 8 indicates that the mixed norm controllers designed for 10 and 20 per cent parametric uncertainty yield comparable performance to the μ controllers designed for 5 per cent uncertainty. Hence, the mixed norm designs provide more robust stability for a given level of performance than the μ controllers. Note that these comparisons are for nominal performance and may not hold for robust performance. In these analyses, the additive uncertainty is held fixed since it is defined with respect to the model and serves only to force the controller to roll off and gain stabilize the high-frequency unmodelled dynamics.

Robust stability of each design is evaluated using mixed μ analysis where the parametric uncertainty is considered real and the additive uncertainty complex. As a result, the mixed μ measure is a less conservative measure of robust stability. Figure 9 plots the μ measure for the set of H_2 controllers for varying authority levels as a function of parametric uncertainty level. This plot should be interpreted as indicating the magnitude of perturbation required to destabilize the closed loop. From equation (14), a μ measure < 1

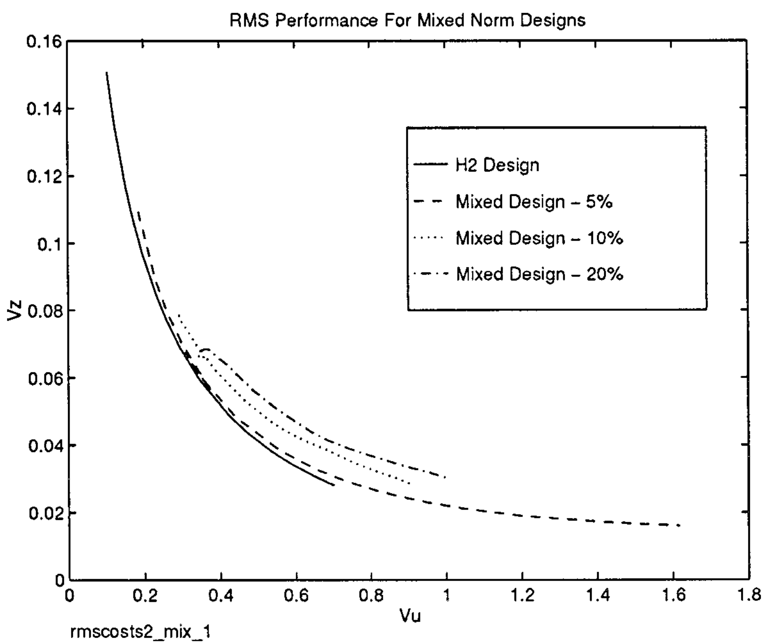

Figure 8. Impact of uncertainty level on RMS performance

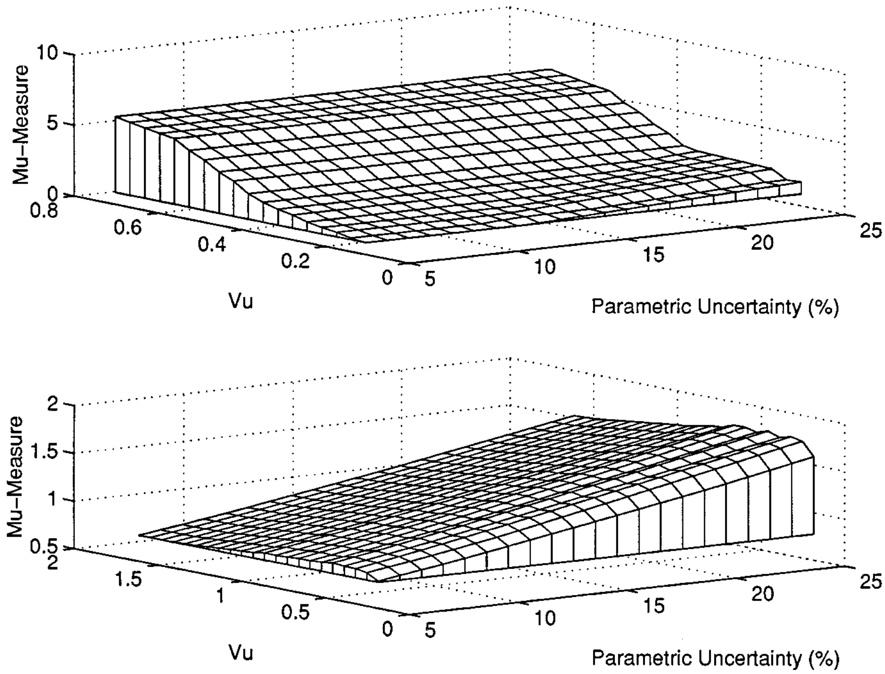

Figure 9. Robust stability analysis of H_2 (top) controllers and mixed norm designs performed for 5 per cent uncertainty (bottom)

indicates robust stability is guaranteed for all plants in the uncertain set. For a controller associated with a μ measure of β, the system will be unstable for $\|\Delta\|_\infty \geqslant 1/\beta$. The H_2 designs are robust with respect to the uncertainty model only for very low authority controllers.

Figure 9 illustrates the well-known property of H_2 controllers that as control authority increases, the sensitivity (in terms of stability) to model error increases. This figure also indicates that the μ measure is relatively insensitive to different levels of parametric uncertainty at high control authority levels which indicates that the additive uncertainty dominates the stability analysis. Only at low authority levels are the H_2 designs sensitive to parametric uncertainty. Since control bandwidth is proportional to the authority level for these H_2 designs, the higher authority controllers interact with and destabilize the unmodeled modes.

Robust stability analyses of the mixed norm designs for 5%, 10%, and 20% parametric uncertainty are shown in Figures 9 and 10. For the 5 per cent uncertainty design, an H_∞ overbound of one was achieved. Although robust stability is not guaranteed for levels of uncertainty above 5 per cent, the μ measure for 25 per cent parametric uncertainty is less than two, which is roughly three times better than the H_2 designs. It is also interesting to note that the μ measure for the mixed norm design is sensitive to differences in parametric uncertainty and is relatively insensitive to the control authority, which is opposite the characteristic of the H_2 designs. As a matter of fact, the μ measure decreases slightly with control authority for the mixed norm designs. Somewhat different behaviour is observed with the mixed norm designs for 10 and 20 per cent parametric uncertainty. The mixed norm design set for 10 parametric uncertainty used an H_∞ overbound of 1·3, so robust stability is not fully guaranteed for 10 per cent variations in the uncertain natural frequency. From Fig. 10, the peak μ measure for 10 per cent parameter uncertainty is 1·26. Similarly for the mixed norm design with 20 per cent parametric uncertainty, an H_∞ overbound of 2·1 was used and the peak μ measure is 1·75. These two designs have a characteristic behaviour more similar to the H_2 designs in that the μ measure is more sensitive to control authority than parametric uncertainty level. However, the variation with control authority is significantly less than the H_2 designs.

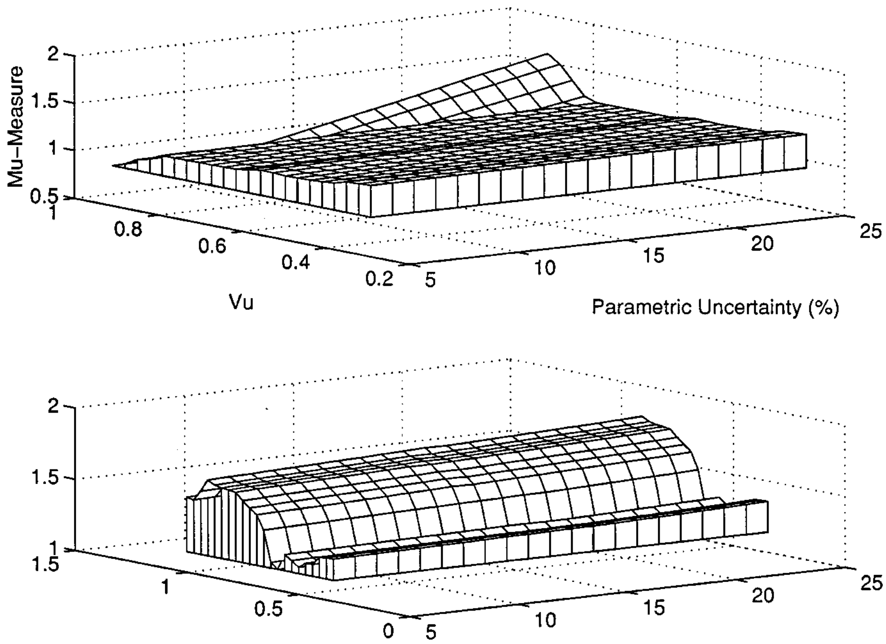

Figure 10. Robust stability analysis of mixed norm designs performed for 10 per cent (top) and 20 per cent uncertainty (bottom)

For a second-order system with an uncertain natural frequency square parameter, (equation (2) with $\delta_2 = 0$), if δ_1 is considered a real parameter the uncertain system will be stable when $\delta_1 > -1$. However, if δ_1 is a complex variation, the system is stable only when $|\delta_1| < 2\zeta$.[21] Thus representing the real parameter uncertainty as a complex variation introduces significant conservatism in the control design. The impact of this is evident in the mixed norm design with 10 and 20 per cent parametric uncertainty. The homotopy began with a fixed-order μ design for T_{z1w1} which exists because of the artificial destabilizing effect of the complex parametric uncertainty. For the 10 per cent uncertainty level, the fixed-order H_∞ design with the D scales from the full order μ design resulted in a minimum H_∞ norm of 1·2539. For 20 per cent uncertainty, the minimum H_∞ norm is 2·0463. Since these designs are for the H_∞ subproblem only, they represent a lower limit on the H_∞ norm for the mixed H_2/μ designs and are used as the initial points for the λ homotopies in the mixed norm designs.

The complex μ measure of each mixed norm boundary controller is only very slightly less than the H_∞ norm overbound, indicating that the D-scales obtained from the full order D–K iteration for T_{z1w1} for each uncertainty level are nearly optimal for the 6th order mixed norm controllers. Had this not been the case, the D-scales could have been optimized for a mixed norm boundary controller, followed by another fixed-order controller optimization step.

Using the simulink model provided with the benchmark problem, the ten evaluation criteria specified in Reference 5 are evaluated for the full order H_2, μ, and fixed (6th) order mixed H_2/μ designs. The performance criteria for the H_2 and mixed H_2/μ controllers, designated by ‘x’ on Figure 7, and the μ controller, designated by ‘o’ on Figure 7, are listed in Table I. The H_2 and mixed H_2/μ design points are for $\rho = 30$ since for $\rho < 25$, the hard constraint on peak control input is violated with the H_2 design. Examination of the time responses for the mixed norm control designs revealed that the constraint was violated only by a small margin of short duration with no discernible impact on closed-loop performance.

To illustrate the level of performance attained by these controller design points, open and closed loop time responses of the relative floor displacements to the Hachinohe Earthquake record are shown in Figures

Table I. Evaluation criteria for controller design points (RMS performance and constraint values computed at the nominal design point, $\omega_g = 14{\cdot}5$ rad/s and $\zeta_g = 0{\cdot}3$, using a simulation duration of 750 s; no maximization over (ω_g, ζ_g) was done.)

Criteria	H_2	μ	Mixed H_2/μ
J1	0·1213	0·1229	0·1226
J2	0·2713	0·2683	0·2734
J3	0·0388	0·0425	0·0395
J4	0·0442	0·0443	0·0436
J5	0·0086	0·0080	0·0087
J6	0·2840	0·2960	0·2818
J7	0·8073	0·8009	0·7902
J8	0·0913	0·0902	0·1030
J9	0·0917	0·0858	0·2112
J10	0·0375	0·0370	0·0396
RMS control force (kN)	2·4717	2·3207	2·5250
RMS control input (V)	0·7395	0·7983	0·7547
RMS actuator disp. (cm)	0·0908	0·0993	0·0925
Peak control force (kN)	10·8500	10·6910	11·4517
Peak control input (V)	2·9973	3·3087	3·5919
Peak actuator disp. (cm)	0·3657	0·3951	0·3912

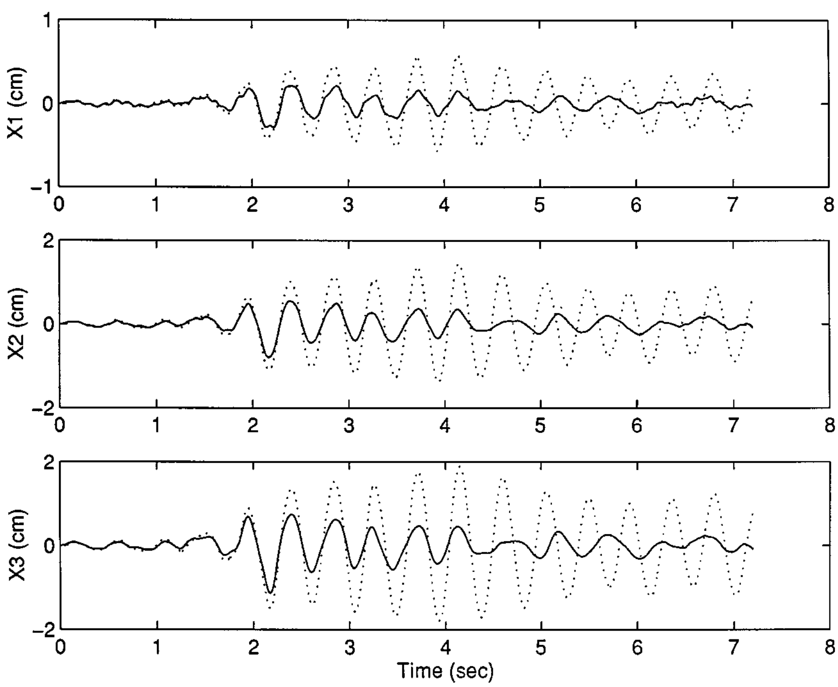

Figure 11. Closed-loop response of H2 controller

11–13. The nominal evaluation model was used with the simulink model to generate these time responses. These figures indicate that the three controller design points yield similar levels of vibration suppression, albeit with different levels of robustness.

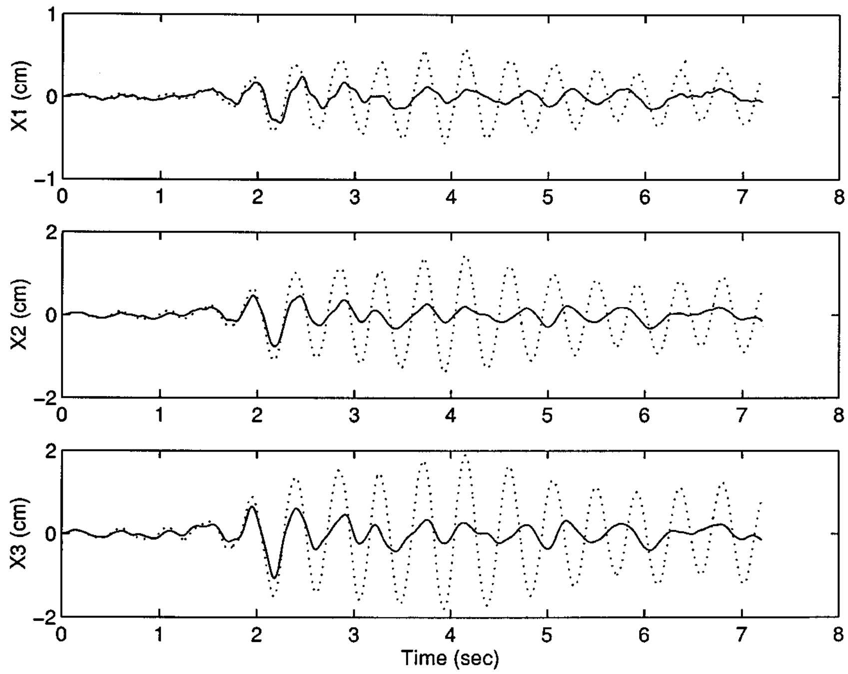

Figure 12. Closed-loop response of μ controller

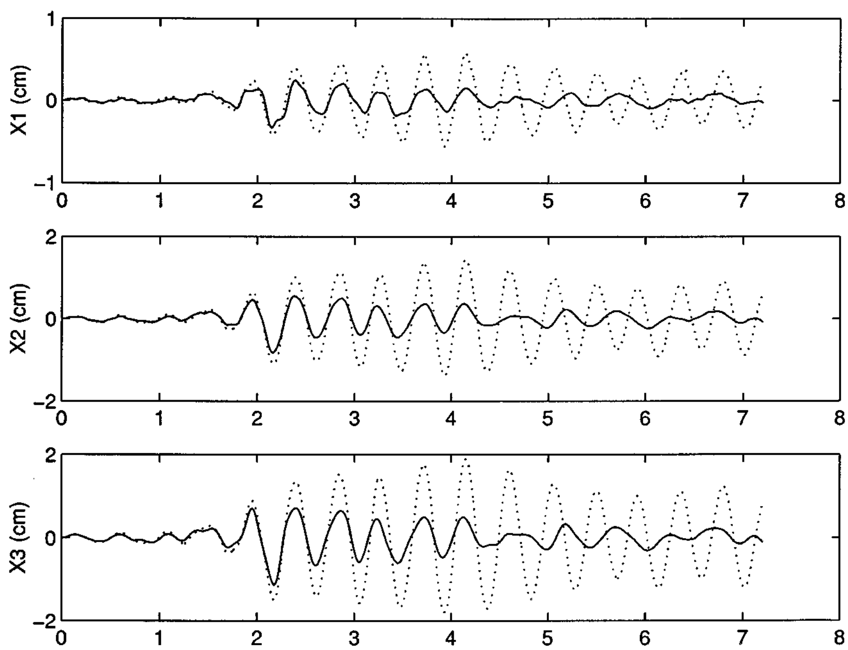

Figure 13. Closed-loop response of mixed norm controller

6. CONCLUSIONS

This paper has presented a comparison of H_2, μ-synthesis, and mixed H_2/μ control design for a structural benchmark control problem with an emphasis on the issues of robust stability and nominal performance. A particular uncertainty model was employed which accounted for uncertainty in the natural frequency of each mode in the control bandwidth and an additive uncertainty to provide stability in the presence of high-frequency unmodelled modes. It has been shown that although H_2 design yields good nominal performance, the designs have poor stability characteristics with respect to errors in the design model. μ-synthesis designs provide robust stability, but tend to sacrifice performance for robust stability and result in controllers with higher control authority than the H_2 designs for a given level of performance. A fixed-order mixed H_2/μ design approach was introduced which provides the same robust stability guarantees as the μ-synthesis designs while almost fully recovering the H_2 nominal performance levels. Accounting for the model errors also permits higher levels of control authority for which the H_2 designs are destabilizing with the evaluation model. This mixed norm design approach was demonstrated to be an effective means for designing H_2 controllers with robust stability for the benchmark structural control problem.

REFERENCES

1. G. W. Housner and A. F. Masri, *Int. Workshop on Struct. Control*, University of Southern California Press, Los Angeles, CA, 1993.
2. W. E. Schmitendorf, F. Jabbari and J. N. Yang, 'Robust control techniques for buildings under earthquake excitations', *Earthquake Engng. Struct. Dyn.* **23**, 539–552 (1994).
3. J. N. Yang, J. C. Wu, A. M. Reinhorn, M. Riley, W. E. Schmitendorf and F. Jabbari, 'Experimental verifications of H_∞ and sliding mode control for seismic excited buildings', *ASCE J. Struct. Engng.* **122**, 69–75.
4. I. E. Kose, W. E. Schmitendorf, F. Jabbari and J. N. Yang, 'Active seismic response control using static output feedback', *ASCE J. Engng. Mech.* **122**, 651–659 (1996).
5. B. F. Spencer, Jr., S. Dyke and H. Deoskar, 'Benchmark problems in structural control', *Proc. 1997 ASCE Structures Congr.*, April 13–16, Portland, OR, 1997.
6. G. J. Balas, and P. M. Young, 'Control design for variations in structural natural frequencies', *J. Guidance, Control, Dyn.* **18**(2), 325–332 (1995).
7. G. D. Sweriduk and A. J. Calise, 'A differential game approach to the mixed H_2/H_∞ problem', *AIAA Paper 94-3660-CP*, August 1994.
8. A. J. Calise and G. D. Sweriduk, 'Active attenuation of building structural response using robust control', *ASCE J. Engng. Mech.*, accepted subject to minor revisions.
9. B. A. Frances, *A Course in H_∞ Control Theory*, Springer, Berlin, 1987.
10. J. C. Doyle, K. Glover, P. Khargonekar and B. A. Francis, 'State-space solutions to standard H_2 and H_∞ control problems', *IEEE Trans. Automat. Control* **34**, 831–847 (1989).
11. J. M. Maciejowski, *Multivariable Feedback Design*, Addison Wesley, Reading, MA, 1989.
12. M. Morari and E. Zafiriou, *Robust Process Control*, Prentice-Hall, Englewood Cliffs, NJ, 1989.
13. J. C. Doyle, 'Analysis of feedback systems with structured uncertainties', *Proc. IEE-D* **129**, 242–250 (1982).
14. J. C. Doyle, 'Lecture notes on advances in multivariable control', *ONR/Honeywell Workshop on Advances in Multivariable Control*, Minneapolis, MN, October, 1984.
15. J. C. Doyle and C. C. Chu, 'Robust control of multivariable and large scale systems', *Final Technical Report for AFOSR*, Contract No. F49620-84-C-0088, March 1986.
16. D. B. Ridgely, R. A. Canfield, D. E. Walker and L. D. Smith, 'The fixed order mixed H_2/H_∞ control problem: development and numerical solution', *Int. J. Robust Nonlinear Control*, submitted for publication.
17. M. S. Whorton, H. Buschek, and A. J. Calise, 'Homotopy algorithm for fixed order mixed H_2/H_∞ design', *J. Guidance, Control, Dyn.* **19**, 1262–1269 (1996).
18. S. L. Richter and R. A. DeCarlo, 'Continuation methods: theory and applications', *IEEE Trans. Circuits Systems*, **CAS-30**, 347–352 (1983).
19. M. S. Whorton, 'High-performance, robust control of flexible space structures', Ph.D. thesis, The Georgia Institute of Technology, 1997.
20. G. J. Balas, J. C. Doyle, K. Glover, A. Packard and R. Smith, *μ-Analysis and Synthesis TOOLBOX*, The Mathworks, 1993.
21. G. J. Balas, 'Robust control of flexible structures: theory and experiments', Ph.D. thesis, The California Institute of Technology, 1990.

